JACS
JOURNAL OF THE AMERICAN CHEMICAL SOCIETY
Communication
pubs.acs.org/JACS

Ordered Porous Pd Octahedra Covered with Monolayer Ru Atoms

Jingjie Ge,[†] Dongsheng He,[†] Lei Bai,[†] Rui You,[†] Haiyuan Lu,[†] Yue Lin,[†] Chaoliang Tan,[∥] Yan-Biao Kang,[†] Bin Xiao,[†] Yuen Wu,[†] Zhaoxiang Deng,[†] Weixin Huang,[†] Hua Zhang,[∥] Xun Hong,*[,†] and Yadong Li*[,†,‡,§]

[†]Center of Advanced Nanocatalysis (CAN), University of Science and Technology of China, Hefei, Anhui 230026, China
[‡]Department of Chemistry and [§]Collaborative Innovation Center for Nanomaterial Science and Engineering, Tsinghua University, Beijing 100084, China
[∥]Center for Programmable Materials, School of Materials Science and Engineering, Nanyang Technological University, 50 Nanyang Avenue, Singapore 639798, Singapore

Supporting Information

ABSTRACT: Monolayer Ru atoms covered highly ordered porous Pd octahedra have been synthesized via the underpotential deposition and thermodynamic control. Shape evolution from concave nanocube to octahedron with six hollow cavities was observed. Using aberration-corrected high-resolution transmission electron microscopy and X-ray photoelectron spectroscopy, we provide quantitative evidence to prove that only a monolayer of Ru atoms was deposited on the surface of porous Pd octahedra. The as-prepared monolayer Ru atoms covered Pd nanostructures exhibited excellent catalytic property in terms of semihydrogenation of alkynes.

Noble metal nanostructures have been intensely investigated because of their fascinating properties and applications in catalysis,[1] electronics,[2] surface-enhanced Raman scattering, and sensors.[3] It is well-documented that the properties of noble metal nanostructures can be tuned by their size, shape, and structures.[4,5] Recently, bimetallic noble metal nanostructures such as heterostructures and core−shell structures have attracted increasing attention as they exhibit enhanced properties and stability arising from the synergistic effect between two metals.[6−8] More importantly, only a fractional amount of noble metal at the surface, such as few atomic layer or monolayer noble metal formed on single crystal metal surfaces, has significantly changed the catalytic and optical properties of the bimetallic nanocrystals.[9−11] For example, based on the theoretical calculation, monolayer Pt atoms on Pd (111) surface can surpass the oxygen reduction reaction activity of pure Pt.[9] Therefore, controlling the surface of bimetallic nanostructures at the atomic level can effectively tune catalytic and optical properties of bimetallic materials.

Moreover, much attention has been paid to the synthesis of hollow or porous noble bimetallic nanostructures as they provide enhanced catalytic properties.[12−15] The main methods for preparation of hollow or porous noble metal nanostructures rely on the removal of sacrificial materials based on the Kirkendall effect, galvanic replacements, or selective etching.[12−15] Although a few bottom-up approaches were developed for the synthesis of porous Au nanostructures with tailorable hollow features,[16] it still remains challenging to control the formation of highly ordered porous structure in a nanoparticle, especially for bimetallic noble metal nanostructures. Herein, for the first time, we synthesize a novel bimetallic nanostructure that is composed of monolayer Ru atoms on highly ordered porous Pd octahedrons, which exhibit excellent performance in catalytic semihydrogenation of alkynes.

In a typical experiment, after K_2PdCl_4 (19.6 mg, 0.06 mmol), $RuCl_3{\cdot}xH_2O$ (12.4 mg, 0.06 mmol) and PVP (120 mg) were dissolved in 15 mL of formaldehyde aqueous solution, the mixture was under magnetic stirring at room temperature for 1 h. Then, the solution was transferred into an autoclave and kept at 130 °C for 2 h. After being washed with water to remove excess PVP, the final product was collected and characterized by aberration-corrected high-resolution transmission electron microscopy (HRTEM). As shown in Figures 1a and S1, the octahedral nanostructures with a longest diameter of about 40.0 ± 4.6 nm were observed. Interestingly, lower contrast near the tips of octahedra clearly shows the hollow cavities with diameter of <5 nm. A high-angle annular dark-field scanning transmission electron microscopy (HAADF-STEM) image (Figure 1b) of the obtained nanostructures shows significantly darker contrast at each tip of the octahedral and six hollow cavities exist in a single nanoparticle. Line-scan energy-dispersive X-ray spectroscopy (EDS) of a single octahedron shows that the less contrast regions in the HAADF-STEM image are due to the absence of Pd (Figure S2). Figure 1c shows the aberration-corrected high-resolution HAADF-STEM image of a tip of the obtained octahedron. The lattice fringes of 0.225 and 0.195 nm were corresponding to the {111} and {200} planes of Pd, respectively. Although only Pd was found in the octahedral nanostructures in the EDS measurement (Figure S3), a weak binding energy peak at 280.7 eV which can be assigned to Ru $3d_{5/2}$ of metallic Ru^0 was detected by the X-ray photoelectron spectroscopy (XPS) spectrum (Figure S4).

To further confirm the presence of Ru, the aberration-corrected HAADF-STEM was used to investigate the obtained octahedral nanostructures at the atomic scale (Figure 1d, e). Note that Ru and Pd have different crystal structures, i.e., hexagonal close-packed (hcp) Ru with stacking sequence of atomic layers expressed as ABAB and face-centered cubic (fcc) Pd with atomic layers cycle between three equivalent shifted positions marked as ABCABC. Both hcp and fcc are close-

Received: August 24, 2015
Published: November 9, 2015

DOI: 10.1021/jacs.5b08956
J. Am. Chem. Soc. 2015, 137, 14566−14569

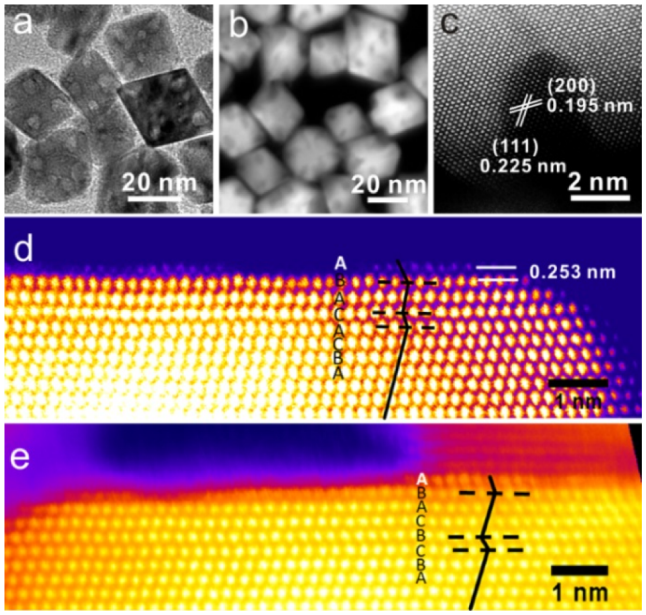

Figure 1. (a) TEM and (b) HAADF-STEM images of ordered porous octahedral nanostructures. Atomic resolution aberration-corrected HAADF-STEM images of (c) the porous area of the ordered porous octahedral nanostructure and (d,e) the surface of octahedra. False color was applied to enhance the contrast.

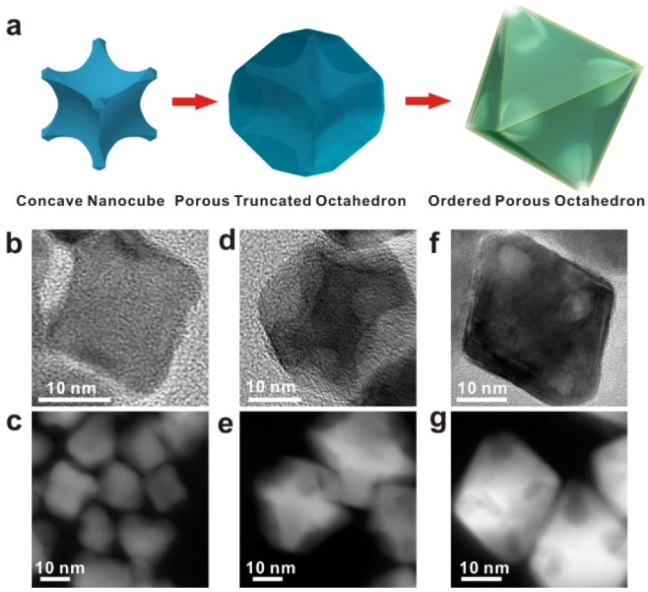

Figure 2. (a) Schematic illustration of the synthesis of ordered porous octahedra. (b,d,f) HRTEM images and (c,e,g) STEM images of concave nanocubes (b,c), porous truncated octahedra (d,e), and final ordered porous octahedra (f,g).

packed structures, while fcc {111} and hcp {001} have the same atom arrangement on their close-packed facets. On those surfaces, the atoms arrange in a triangle fashion to maximize the packing density (indicated by the shadow area in Figure S5a-b). Ru {001} and Pd {111} show a moderate lattice mismatch of 3.6% on the close-packed facet, which enables the deposition of Ru on Pd {111} surface. However, stack faults have been observed near the surface. For example, the stacking sequence is ABAC (from the topmost layer downward), while the second topmost layer forms a mirror layer, i.e., a twin boundary (Figures 1d-e, S6). More importantly, the topmost layer always occupies the hcp sites (with respect to the substrate). This is a very clear sign of the deposition of hcp Ru on the surface of Pd. The hcp-to-fcc phase transition existing near the surface might result in the formation of stack faults.[8] In addition, the plane distance between the topmost layer and the second topmost layer is 2.53 Å, which is significantly larger than the interlayer distance of Ru (2.15 Å, Figure S5d). This result confirms that a monolayer rather than bilayer of Ru atoms was deposited on the surface of Pd octahedron.

Moreover, XPS and aberration-corrected HAADF-STEM results provide quantitative evidence that only a monolayer of Ru atoms was deposited on Pd surface. The introduction of Ru ions during the growth of Pd is an effective strategy to control the morphology of Pd nanoparticle. Only solid nanoparticles were obtained without the presence of Ru^{3+} (Figure S6). These features match well with the underpotential deposition (UPD) process, which refers to the deposition of a metal monolayer on a foreign metal substrate at a potential much more positive than that for deposition on the same metal surface.[17,18] The UPD process has been widely used to direct the growth of different shaped noble metal nanocrystals like Au octahedra,[19] Au nanorods,[20] Au–Pd alloy hexoctahedra,[21] and Pd concave nanostructures,[22,23] although the deposited monolayer was rarely detected.

Figure 2a schematically illustrates the morphological evolution of the ordered porous nanostructures. First, the concave nanocube with diameter of 15 nm was obtained at room temperature for 1 h (Figure 2b-c). Then, by increasing the reaction temperature to 130 °C, the truncated octahedron nanoparticle with darker contrast at the center and lighter contrast at the surface was obtained after the reaction for 15 min (Figure 2d-e). The size and shape of darker contrast part are similar to the concave nanocube (Figure 2b), while the less contrast part in the HRTEM and STEM image might be due to the generated hollow cavities. As the reaction continues for 2 h, six hollow cavities formed at the surface of concave nanocube remained in the well-defined octahedral nanocrystals (Figure 2f-g). The shape evolution from cube to octahedron is similar to the reported Ag, Au, and Pt nanocrystals by using PVP as a surface-capping agent under thermodynamic control.[24]

To the best of our knowledge, the obtained porous Pd octahedra covered with monolayer Ru atoms is a novel nanostructure. The unique porous structure with trace amounts of Ru on the surface might possess enhanced catalytic properties. As a proof-of concept application, its catalytic performance for the semihydrogenation of alkynes was investigated. Traditionally, alkenes were obtained through the semihydrogenation of alkynes using the Lindlar catalyst (Pd/$CaCO_3$ and $Pb(OAc)_2$, in conjunction with quinolone).[25] Unfortunately, the alkynes were easily overhydrogenated to obtain alkanes, and the use of $Pb(OAc)_2$ is environmentally unfriendly.[26] Figures 3a-b and S7a-b show the performance of semihydrogenation of phenylacetylene catalyzed by using the obtained porous Pd octahedra covered with monolayer Ru atoms. Promisingly, 100% conversion of phenylacetylene and 90% of styrene selectivity were obtained in 4 h. In a control experiment, the yield of phenylacetylene was only 43% when the same amount of Pd nanoparticles was used as the catalyst (Figure S8).

DOI: 10.1021/jacs.5b08956
J. Am. Chem. Soc. 2015, 137, 14566–14569

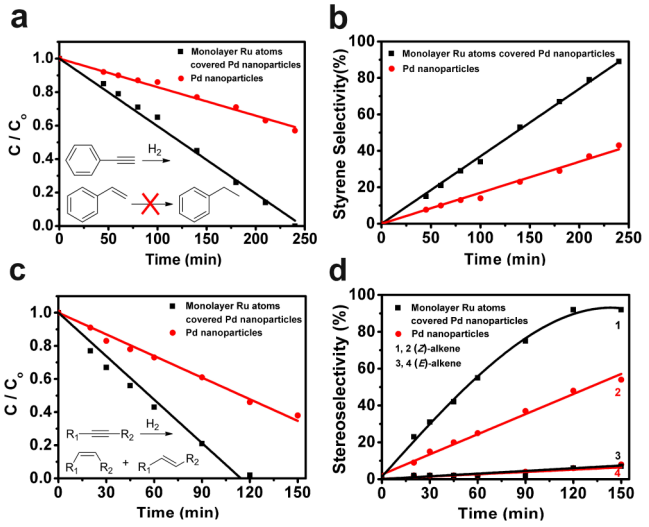

Figure 3. Catalytic semihydrogenation of alkynes. (a) Conversion of phenylacetylene and (b) selectivity of styrene catalyzed by the porous Pd octahedra covered with monolayer Ru atoms nanoparticles and the Pd nanoparticles. (c) Conversion of methyl non-2-ynoate (R_1 = C_6H_{13}, R_2 = CO_2Me) to (d) (*Z*)-methyl non-2-enoate (curve 1 and 2) and (*E*)-methyl non-2-enoate (curve 3 and 4) catalyzed by the porous Pd octahedra covered with monolayer Ru atoms nanoparticles and the Pd nanoparticles. See Supporting Information for details.

To further study the activity and stereoselectivity of the as prepared porous Pd octahedra covered with monolayer Ru atoms, the catalytic performance was studied by the semihydrogenation of internal alkyne. The result showed that the conversion of methyl non-2-ynoate was >99% after 2 h catalysis reaction by using the porous Pd octahedra covered with monolayer Ru atoms, while 56% conversion with the same amount of Pd nanoparticles as the catalyst (Figure 3c). Moreover, the porous Pd octahedra covered with monolayer Ru atoms gave excellent selectivity (92%) of (*Z*)-methyl non-2-enoate, and the stereoselectivity could be maintained and even prolong the reaction time after non-2-ynoate disappeared (Figures 3d and S7c-d). Importantly, the over-reduction product, i.e., methyl nonanoate, was not detected during the reaction. The stability of the porous Pd octahedra covered with monolayer Ru atoms was conducted by a recycling test. No obvious change was observed for the activity and selectivity throughout four cycles (Figure S9). The TEM image of the porous Pd octahedra covered with monolayer Ru atoms catalyst after four catalytic cycles shows that the catalysts are still well-dispersed and their shape is well-preserved (Figure S10).

Therefore, the monolayer Ru atoms covered porous Pd octahedral nanoparticle is an excellent catalyst, whose specific activity is about 5 times higher than that of the Pd catalyst (see Figure S11 for details). The high selectivity of alkenes could be ascribed to the synergistic effects between the monolayer Ru atoms and the porous Pd nanocrystals. As known, ruthenium catalysts usually form a stable catalyst−substrate complex in the hydrogenation of alkynes,[27,28] and thus the active sites on the surface of catalysts could be blocked by the occupied Ru−substrate complex. The role of the covered Ru atoms is similar to the generally accepted poisoning effect of the Lindlar catalyst.[25,29]

In summary, for the first time, we reported the preparation of a novel nanostructure, i.e., porous Pd octahedra covered with monolayer Ru atoms nanocrystals. Taking the advantage of underpotential deposition and thermodynamic control, the Pd octahedral nanocrystals with six hollow cavities were generated from the Pd concave nanocubes. Stack faults near the surface of nanocrystals were observed, and the monolayer of Ru atoms always occupy the hcp sites. These novel bimetallic nanocrystals exhibited excellent catalytic activity and stereoselectivity for the semihydrogenation of alkynes.

■ ASSOCIATED CONTENT

Supporting Information

The Supporting Information is available free of charge on the ACS Publications website at DOI: 10.1021/jacs.5b08956.

Detailed experimental procedures; HAADF-STEM images; EDS and XPS spectrum of the monolayer of porous Pd octahedral covered with Ru atoms nanoparticles (PDF)

■ AUTHOR INFORMATION

Corresponding Authors

*hongxun@ustc.edu.cn

*ydli@mail.tsinghua.edu.cn

Notes

The authors declare no competing financial interest.

■ ACKNOWLEDGMENTS

This work was supported by the Fundamental Research Funds for the Central Universities (WK2060190042), and the National Natural Science Foundation of China (21571169). H.Z. thanks the financial support from MOE under AcRF Tier 2 (ARC 26/13, no. MOE2013-T2-1-034; ARC 19/15, no. MOE2014-T2-2-093) and AcRF Tier 1 (RGT18/13, RG5/13), and NTU under Start-Up Grant (M4081296.070.500000) in Singapore.

■ REFERENCES

(1) Corma, A.; Concepción, P.; Boronat, M.; Sabater, M. J.; Navas, J.; Yacaman, M. J.; Larios, E.; Posadas, A.; López-Quintela, M. A.; Buceta, D.; Mendoza, E.; Guilera, G.; Mayoral, A. *Nat. Chem.* **2013**, *5*, 775.

(2) Smith, P. A.; Nordquist, C. D.; Jackson, T. N.; Mayer, T. S.; Martin, B. R.; Mbindyo, J.; Mallouk, T. E. *Appl. Phys. Lett.* **2000**, *77*, 1399.

(3) Mulvihill, M. J.; Ling, X. Y.; Henzie, J.; Yang, P. *J. Am. Chem. Soc.* **2010**, *132*, 268.

(4) Xia, Y.; Xiong, Y.; Lim, B.; Skrabalak, S. E. *Angew. Chem., Int. Ed.* **2009**, *48*, 60.

(5) Hong, X.; Tan, C.; Chen, J.; Xu, Z.; Zhang, H. *Nano Res.* **2015**, *8*, 40.

(6) Wang, D.; Li, Y. *Adv. Mater.* **2011**, *23*, 1044.

(7) Fan, Z.; Zhu, Y.; Huang, X.; Han, Y.; Wang, Q.; Liu, Q.; Huang, Y.; Gan, C. L.; Zhang, H. *Angew. Chem., Int. Ed.* **2015**, *54*, 5672.

(8) Hsieh, Y.-C.; Zhang, Y.; Su, D.; Volkov, V.; Si, R.; Wu, L.; Zhu, Y.; An, W.; Liu, P.; He, P.; Ye, S.; Adzic, R. R.; Wang, J. X. *Nat. Commun.* **2013**, *4*, 2466.

(9) Zhang, J.; Vukmirovic, M. B.; Xu, Y.; Mavrikakis, M.; Adzic, R. R. *Angew. Chem., Int. Ed.* **2005**, *44*, 2132.

(10) Gong, K.; Su, D.; Adzic, R. R. *J. Am. Chem. Soc.* **2010**, *132*, 14364.

(11) Yang, Y.; Liu, J.; Fu, Z.-W.; Qin, D. *J. Am. Chem. Soc.* **2014**, *136*, 8153.

(12) Gonzalez, E.; Arbiol, J.; Puntes, V. F. *Science* **2011**, *334*, 1377.

(13) Hong, X.; Wang, D.; Cai, S.; Rong, H.; Li, Y. *J. Am. Chem. Soc.* **2012**, *134*, 18165.

(14) Chen, C.; Kang, Y.; Huo, Z.; Zhu, Z.; Huang, W.; Xin, H. L.; Snyder, J. D.; Li, D.; Herron, J. A.; Mavrikakis, M.; Chi, M.; More, K.

DOI: 10.1021/jacs.5b08956
J. Am. Chem. Soc. 2015, 137, 14566−14569

L.; Li, Y.; Markovic, N. M.; Somorjai, G. A.; Yang, P.; Stamenkovic, V. R. *Science* **2014**, *343*, 1339.
(15) Wu, Y.; Wang, D.; Zhou, G.; Yu, R.; Chen, C.; Li, Y. *J. Am. Chem. Soc.* **2014**, *136*, 11594.
(16) Langille, M. R.; Personick, M. L.; Zhang, J.; Mirkin, C. A. *J. Am. Chem. Soc.* **2011**, *133*, 10414.
(17) Herrero, E.; Buller, L. J.; Abruna, H. D. *Chem. Rev.* **2001**, *101*, 1897.
(18) Grzelczak, M.; Pérez-Juste, J.; Mulvaney, P.; Liz-Marzán, L. M. *Chem. Soc. Rev.* **2008**, *37*, 1783.
(19) Personick, M. L.; Langille, M. R.; Zhang, J.; Mirkin, C. A. *Nano Lett.* **2011**, *11*, 3394.
(20) Jackson, S. R.; McBride, J. R.; Rosenthal, S. J.; Wright, D. W. *J. Am. Chem. Soc.* **2014**, *136*, 5261.
(21) Zhang, L.; Zhang, J.; Kuang, Q.; Xie, S.; Jiang, Z.; Xie, Z.; Zheng, L. *J. Am. Chem. Soc.* **2011**, *133*, 17114.
(22) Niu, W.; Zhang, W.; Firdoz, S.; Lu, X. *Chem. Mater.* **2014**, *26*, 2180.
(23) Long, R.; Rao, Z.; Mao, K.; Li, Y.; Zhang, C.; Liu, Q.; Wang, C.; Li, Z.-Y.; Wu, X.; Xiong, Y. *Angew. Chem., Int. Ed.* **2015**, *54*, 2425.
(24) Tao, A. R.; Habas, S.; Yang, P. *Small* **2008**, *4*, 310.
(25) Lindlar, H. *Helv. Chim. Acta* **1952**, *35*, 446.
(26) Chinchilla, R.; Nájera, C. *Chem. Rev.* **2014**, *114*, 1783.
(27) Schleyer, D.; Niessen, H. G.; Bargon, J. *New J. Chem.* **2001**, *25*, 423.
(28) Kang, X.; Zuckerman, N. B.; Konopelski, J. P.; Chen, S. *J. Am. Chem. Soc.* **2012**, *134*, 1412.
(29) McEwen, A. B.; Guttieri, M. J.; Maier, W. F.; Laine, R. M.; Shvo, Y. *J. Org. Chem.* **1983**, *48*, 4436.

DOI: 10.1021/jacs.5b08956
J. Am. Chem. Soc. 2015, 137, 14566−14569